

Asymmetric Hysteresis Loops and Horizontal Loop Shifts in Purely Ferromagnetic Nanoparticles [†]

Joscha Detzmeier, Kevin Königer and Andrea Ehrmann *

Faculty of Engineering and Mathematics, Bielefeld University of Applied Sciences, Bielefeld 33619, Germany; joscha.detzmeier@fh-bielefeld.de (J.D.); kevin.koeniger@fh-bielefeld.de (K.K.)

* Correspondence: andrea.ehrmann@fh-bielefeld.de

[†] Presented at the 2nd International Online-Conference on Nanomaterials, 15–30 November 2020; Available online: <https://iocn2020.sciforum.net/>.

Published: 15 November 2020

Abstract: Horizontally shifted and asymmetric hysteresis loops are often associated with exchange-biased samples, consisting of a ferromagnet exchange-coupled with an antiferromagnet. In purely ferromagnetic samples, such effects can occur due to undetected minor loops or thermal effects. Simulations of ferromagnetic nanostructures at zero temperature with sufficiently large saturation fields should not lead to such asymmetries. Here we report on micromagnetic simulations at zero temperature, performed on sputtered nanoparticles with different shapes. The small deviations of the systems due to random anisotropy orientations in the different grains can not only result in strong deviations of magnetization reversal processes and hysteresis loops, but also to distinctly asymmetric, horizontally shifted hysteresis loops in purely ferromagnetic nanoparticles.

Keywords: pseudo-exchange bias; minor loop; micromagnetic simulation; OOMMF; spintronics

1. Introduction

The exchange bias (EB) effect describes a phenomenon that occurs in ferromagnet/antiferromagnet systems due to an exchange coupling at the interface and leads to a shift of the hysteresis loop, often in combination with an asymmetry of the loop [1]. After firstly being found in Co/CoO core/shell nanoparticles [2], the exchange bias is now mostly investigated in thin-film systems [3–6]. Technologically, the effect is particularly relevant for hard disk read heads, spin valves and other spintronic devices [7–10].

Although the origin of the EB is not yet fully understood quantitatively, there is general agreement that the interface between a ferromagnet and an antiferromagnet—or ferrimagnet—plays a crucial role in this effect [11–13]. Recently, the additional influence of long-range interactions in the antiferromagnet has been shown [14,15]. On the other hand, this means that in purely ferromagnetic systems, regardless of size or shape, neither a shift of the hysteresis loop nor an asymmetry of the hysteresis loop is to be expected.

Nevertheless, only few studies report on such effects. In particular, magnetization measurements using the magneto-optical Kerr effect (MOKE), where only magnetization differences are detectable while the absolute magnetization cannot be measured, do not show a possible vertical shift of the hysteresis loop, so that this method is prone to erroneously measuring minor loops that appear to be completely closed, while saturation is not yet reached [16]. On the other hand, exchange bias-like loop shifts were reported in pure antiferromagnets, where they were attributed to uncompensated spins inside the antiferromagnet, which led to field-resistant magnetization [17].

Here we show micromagnetic simulations using the Object Oriented MicroMagnetic Framework (OOMMF) at zero temperature, performed on symmetrical sputtered nanoparticles with different

shapes and holes or slits inside. Such structures are interesting since they can often be used to prepare quaternary memory devices in which two (or even more) bits can be stored in one storage position [18]. Our results show that not only the small deviations of the investigated systems due to random anisotropy orientations in the different grains can lead to strong deviations of magnetization reversal processes and hysteresis loops, but that distinctly asymmetric, horizontally shifted hysteresis loops can occur in a purely ferromagnetic nanoparticle.

2. Materials and Methods

Different nanostructures were modeled, as depicted in Figure 1. The lateral dimensions of the frames are always 100 nm × 100 nm, the height was defined with 10 nm.

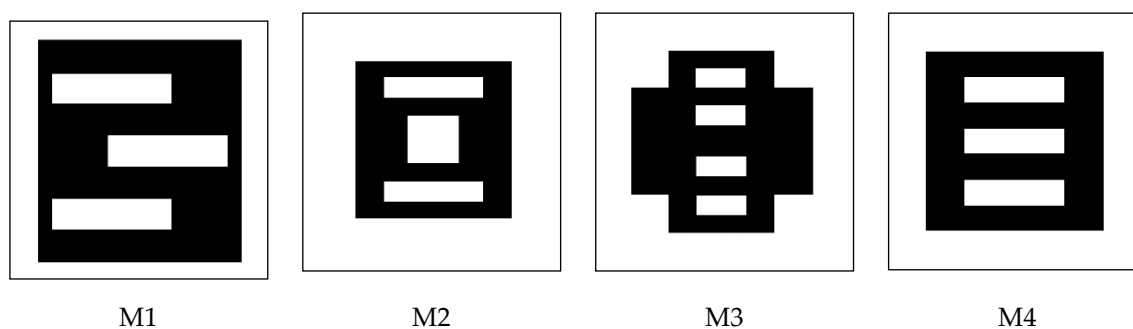


Figure 1. Different masks with slots under investigation. Black areas depict Fe, while white areas are air.

For the simulations OOMMF was used [19], which is based on finite differences for the meshing and dynamic solution of the Landau-Lifshitz-Gilbert (LLG) equation of motion [20]. The material parameters were chosen as typical literature values for iron (Fe): magnetization at saturation $M_s = 1700 \cdot 10^3$ A/m, exchange constant $A = 21 \cdot 10^{-12}$ J/m, magneto-crystalline anisotropy constant $K_1 = 48 \cdot 10^3$ J/m³.

Since such nanostructures are usually fabricated by electron beam lithography [21], the anisotropy axes in neighboring cubic cells of the dimension (5 nm³) were randomly selected so that the configurational anisotropy dominates the magnetization reversal [22]. Setting the Gilbert damping constant $\alpha = 0.5$ results in simulations of a realistic quasi-static case. External magnetic fields were applied in the sample plane and were swept between different maximum fields at diverse angles.

It must be mentioned that the temperature was set to 0 K to avoid thermal fluctuations which could hinder the magnetization reversal process.

3. Results and Discussion

The original goal of this study was to investigate possible structures for quaternary storage applications. Figure 2 shows this effect exemplarily for mask M1 under an angle of 0° (horizontal orientation in Figure 1). Figure 2a depicts the longitudinal magnetization component M_L , parallel to the external magnetic field. Here, the field sweep was stopped only for the widest steps, decreasing the external magnetic field to 0 in order to investigate the stability of the different states achieved in this way at remanence. Thus, in addition to the common two states, two further stable states at remanence could be verified. The snapshots corresponding to the numbers of the intermediate states in Figure 2a are depicted in Figure 2b.

Here it becomes clear why this nanoparticle structure is well-suited to provide more than one stable state at remanence: The four different parts of the structure do not switch the magnetization simultaneously, and these partially switched states correspond to the steps along the slope of the hysteresis loop (Figure 2a).

However, it must be mentioned that the other steps are either not correlated with stable intermediate states (not shown here) or are too narrow to be technologically important and therefore have not been further investigated here. Nevertheless, the different slit positions allow interesting magnetic states and should therefore be examined more in detail in the near future by varying all dimensions of the nanoparticles.

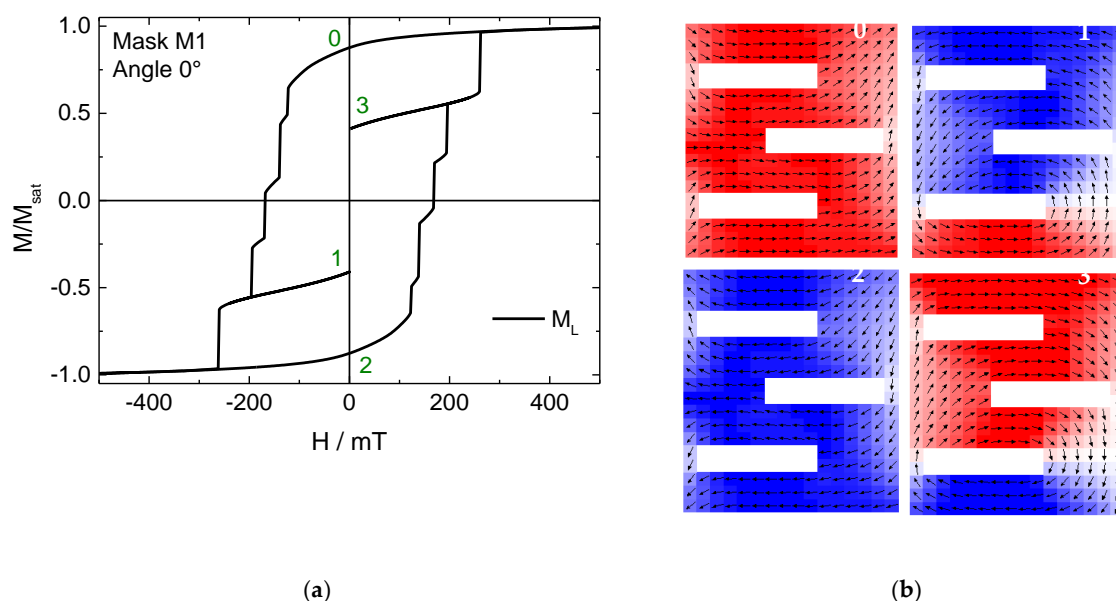


Figure 2. (a) Hysteresis loop and (b) snapshots of stable intermediate states # 0-3, simulated for mask M1 under a field angle of 0° .

A very similar effect is found in mask M4, as shown in Figure 3. Here, each bar switches successively, which theoretically enables even eight different states at remanance. The narrower steps, however, were again not tested because they are technologically less relevant.

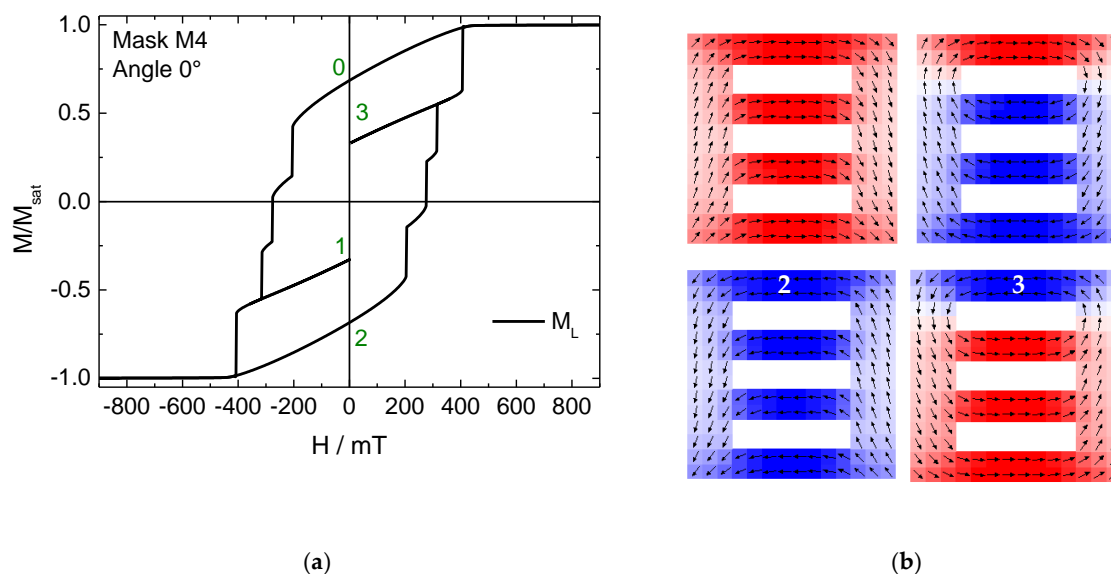


Figure 3. (a) Hysteresis loop and (b) snapshots of stable intermediate states # 0-3, simulated for mask M4 under a field angle of 0° .

Similar effects were found for sample M2 at an angle of 0° . However, the rotation of the external magnetic field to an orientation of 90° led to an unexpected finding. As Figure 4a shows, in this case a horizontally shifted, asymmetric hysteresis curve occurs, which shows the typical form of, e.g., Fe/MnF₂ thin film exchange bias systems [23]. As discussed above, in the case of a pure ferromagnet such a finding should be attributed to the measurement of a minor loop.

While the maximum fields of ± 1 T applied here are already quite large, it is known that saturation fields can be much larger than coercive fields; therefore, therefore, a maximum field of 10 T was applied in the next simulations. This order of magnitude is accessible with common magnets in cryostats. Two of the results are shown in Figure 4b,c. Both experiments yielded symmetrical curves; however,

with different coercive fields and also different magnetization reversal processes, as the strongly different transverse hysteresis loops M_T show. It should be mentioned that Figure 4a contains elements of both hysteresis loops simulated for 10 T maximum fields, underlining the idea that Figure 4a shows a pseudo-EB due to simulating a minor loop.

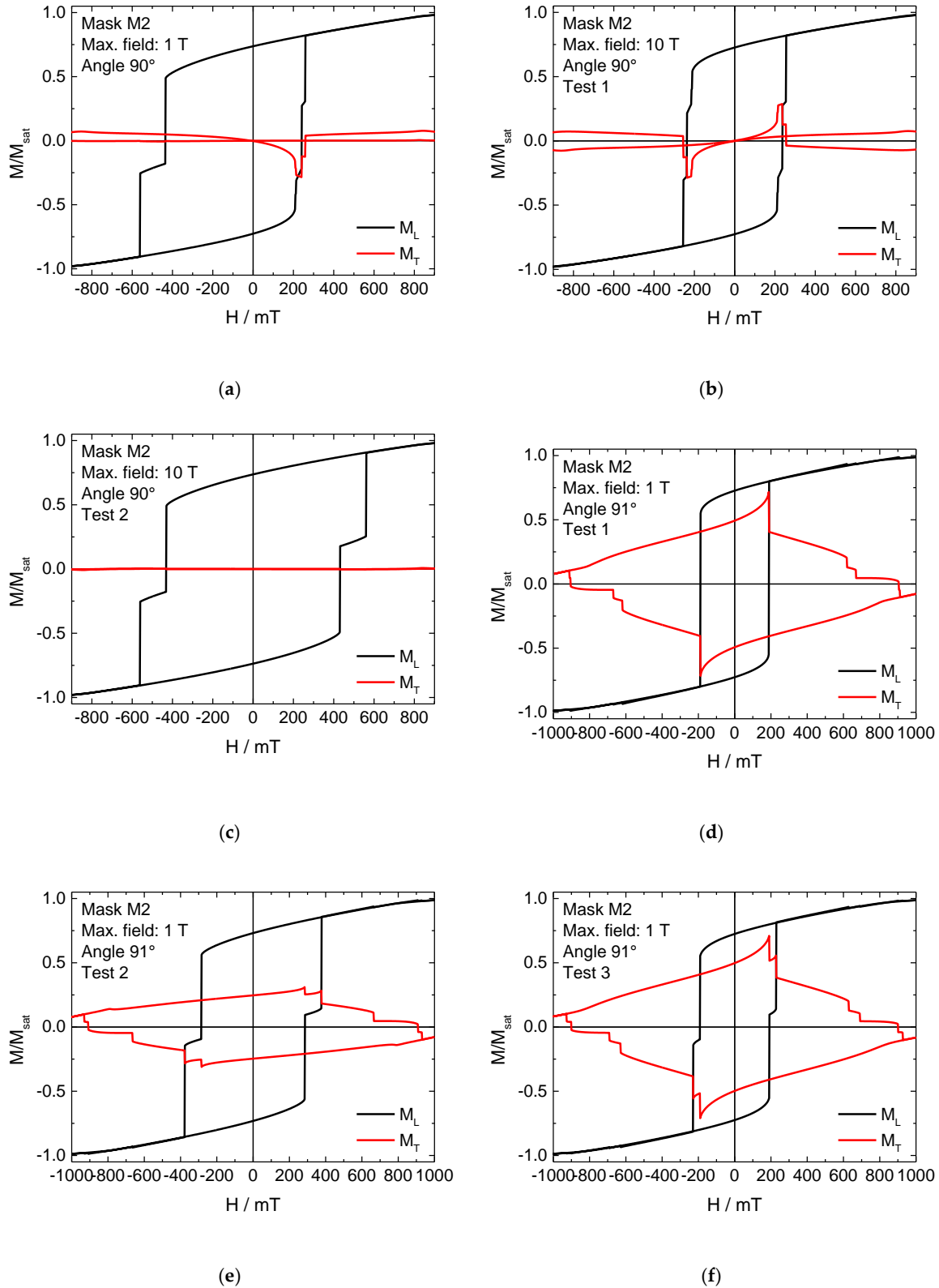


Figure 4. (a–f) Longitudinal and transverse hysteresis loops M_L and M_T , simulated for mask M2 under a field angle of $\sim 90^\circ$ applying different maximum fields, incl. different runs with a maximum external magnetic field of 10 T.

Next, it was tested whether a slight symmetry breaking by a further rotation of the particle 1° would increase the reproducibility of the results. However, as depicted in Figure 4c–f, this approach was not successful. All longitudinal as well as transverse magnetization components differ clearly. It is also visible that the transverse magnetization components are saturated only at absolute fields greater than 900 mT, whereas the longitudinal loops seem to be saturated at less than half of these fields. This underlines the earlier finding that minor loops can remain undiscovered in experiments where the transverse magnetization components are often not measured [16], and again shows the lack of reproducibility of magnetization reversal processes in nanoparticles with small regions that can remain unchanged. Very similar results were found in the sample M3 at an angle of 0° (not shown here), where three different magnetization reversal processes were also observed in subsequent simulations.

While the lack of reliability in some of the samples is problematic for a possible technological application, the pseudo-exchange bias depicted in Figure 4 is even technologically relevant. It has to be emphasized that although this effect shows a similar behavior to exchange bias, it is not due to exchange coupling between different magnetic materials and therefore cannot be considered as exchange bias, but is based on minor loops. Such minor loops are usually avoided in most measurements, since they can lead to misinterpretations. However, the possibility to prepare a purely ferromagnetic system with a pseudo-EB could offer new possibilities to create simpler spin-valves and other spintronics elements that normally require many layers, including a ferromagnetic layer pinned by an antiferromagnet to increase its switching field. If it is possible to prepare layers with an intrinsic pseudo-EB due to geometric constrictions, the antiferromagnet can be omitted and thus spintronics devices can be produced from simpler layer stacks.

4. Conclusion

Different magnetic iron nanostructures with slits proved to be applicable as quaternary storage devices, exhibiting four or even more stable magnetic states at remanence. In two of these structures, strongly varying magnetization reversal processes also occurred, depending on the anisotropy axis distribution in the cells of the meshed sample.

While this behavior can cause problems in the technological application of such magnetic nanostructures, the additional observation of a pseudo-exchange bias in one of the purely ferromagnetic structures suggests the design of ferromagnetic nanostructures with geometric constrictions that leave part of the structure unchanged while the residual magnetization is reversed, thus working similar to the interaction between ferromagnetic and antiferromagnetic layer in an exchange bias system without the need to apply an additional antiferromagnet.

Author Contributions: Conceptualization, J.D., K.K., and A.E.; investigation, J.D. and K.K.; writing—original draft preparation, A.E.; writing—review and editing, J.D. and K.K. All authors have read and agreed to the published version of the manuscript.

Funding: This research received no external funding.

Conflicts of Interest: The authors declare no conflict of interest.

References

1. Morales, T.; Basaran, A.C.; Villegas, J.E.; Navas, D.; Soriano, N.; Mora, B.; Redondo, C.; Batlle, X.; Schuller, I.K. Exchange-Bias Phenomenon: The Role of the Ferromagnetic Spin Structure. *Phys. Rev. Lett.* **2015**, *114*, 097202.
2. Meiklejohn, W.P.; Bean, C.P. New magnetic anisotropy. *Phys. Rev.* **1956**, *102*, 1413.
3. Koon, N.C. Calculations of exchange bias in thin films with ferromagnetic/antiferromagnetic interfaces. *Phys. Rev. Lett.* **1997**, *78*, 4865.
4. Blachowicz, T.; Tillmanns, A.; Fraune, M.; Ghadimi, R.; Beschoten, B.; Güntherodt, G. Exchange bias in epitaxial CoO/Co bilayers with different crystallographic symmetries. *Phys. Rev. B* **2007**, *75*, 054425.
5. O'Grady, K.; Fernancez-Outon, L.E.; Vallejo-Fernandez, G. A new paradigm for exchange bias in polycrystalline thin films. *J. Magn. Magn. Mater.* **2010**, *322*, 883–899.

6. Ehrmann, A.; Blachowicz, B. Angle and rotational direction dependent horizontal loop shift in epitaxial Co/CoO bilayers on MgO(100). *AIP Adv.* **2017**, *7*, 115223.
7. Parkin, S.; Jiang, X.; Kaiser, C.; Panchula, A.; Roche, K.; Samant, M. Magnetically engineered spintronic sensors and memory. *Proc. IEEE* **2003**, *91*, 661–680.
8. Anh Nguyen, T.N.; Fang, Y.; Fallahi, V.; Benatmane, N.; Mohseni, S.M.; Dumas, R.K.; Akerman, J. [Co/Pd]–NiFe exchange springs with tunable magnetization tilt angle. *Appl. Phys. Lett.* **2011**, *98*, 172502.
9. Bonfirm, M.; Ghiringhelli, G.; Montaigne, F.; Pizzini, S.; Brookes, N.B.; Petroff, F.; Vogel, J.; Camarero, J.; Fontaine, A. Element-selective nanosecond magnetization dynamics in magnetic heterostructures. *Phys. Rev. Lett.* **2001**, *86*, 3646.
10. Gasi, T.; Nayak, A.K.; Winterlik, J.; Ksenofontov, V.; Adler, P.; Nicklas, M.; Felser, C. Exchange-spring like magnetic behavior of the tetragonal Heusler compound Mn₂FeGa as a candidate for spin-transfer torque. *Appl. Phys. Lett.* **2013**, *102*, 202402.
11. Meiklejohn, W.H. Exchange anisotropy—A review. *J. Appl. Phys.* **1962**, *33*, 1328.
12. Nogués, J.; Schuller, I.K. Exchange bias. *J. Magn. Magn. Mater.* **1999**, *192*, 203–232.
13. Beschoten, B.; Keller, J.; Tillmanns, A.; Güntherodt, G. Domain state model for exchange bias: Training effect of diluted Co_{1-y}O on exchange bias in Co-CoO. *IEEE Trans. Magn.* **2002**, *38*, 2744–2746.
14. Morales, R.; Li, Z.-P.; Olamit, J.; Liu, K.; Alameda, J.M.; Schuller, I.K. Role of the antiferromagnetic Bulk spin structure on exchange bias. *Phys. Rev. Lett.* **2009**, *102*, 097201.
15. Khan, M.Y.; Wu, C.-B.; Kuch, W. Pinned magnetic moments in exchange bias: Role of the antiferromagnetic bulk spin structure. *Phys. Rev. B* **2014**, *89*, 094427.
16. Ehrmann, A.; Komraus, S.; Blachowicz, T.; Domino, K.; Nees, M.K.; Jakobs, P.J.; Leiste, H.; Mathes, M.; Schaarschmidt, M. Pseudo exchange bias due to rotational anisotropy. *J. Magn. Magn. Mater.* **2016**, *412*, 7–10.
17. Henne, B.; Ney, V.; de Souza, M.; Ney, A. Exchange-bias-like effect of an uncompensated antiferromagnet. *Phys. Rev. B* **2016**, *93*, 144406.
18. Yoo, T.H.; Khym, S.; Yea, S.-Y.; Lee, S.H.; Liu, X.; Furdyna, J.K. Four discrete Hall resistance states in single-layer Fe film for quaternary memory devices. *Appl. Phys. Lett.* **2009**, *95*, 202505.
19. Donahue, M.J.; Porter, D.G. *OOMMF User's Guide, Version 1.0*; Interagency Report NISTIR 6376; National Institute of Standards and Technology: Gaithersburg, MD, USA, 1999.
20. Gilbert, T.L. A phenomenological theory of damping in ferromagnetic materials. *IEEE Trans. Magn.* **2004**, *40*, 3443.
21. Sudsom, D.; Juhász Junger, I.; Döpke, C.; Blachowicz, T.; Hahn, L.; Ehrmann, A. Micromagnetic simulation of vortex development in magnetic bi-material bow-tie structures. *Cond. Matter* **2020**, *5*, 5.
22. Cowburn, R.P.; Adeyeye, A.O.; Welland, M.E. Configurational anisotropy in nanomagnets. *Phys. Rev. Lett.* **1998**, *81*, 5414.
23. Tillmanns, A.; Oertker, S.; Beschoten, B.; Güntherodt, G.; Leighton, C.; Schuller, I.K.; Nogués, J. Magneto-optical study of magnetization reversal asymmetry in exchange bias. *Appl. Phys. Lett.* **2006**, *89*, 202512.

Publisher's Note: MDPI stays neutral with regard to jurisdictional claims in published maps and institutional affiliations.



© 2020 by the authors. Submitted for possible open access publication under the terms and conditions of the Creative Commons Attribution (CC BY) license (<http://creativecommons.org/licenses/by/4.0/>).